



OPEN A novel breath pattern model and analysis to minimize patient discomfort in medical ventilators

M. Deepa¹✉, R. Vidhyapriya² & A. S. Raagul³

Typical waveforms used for the simulation of pressure and volume-controlled ventilation in medical ventilators have been extensively studied in the literature. The majority of simulation studies reported employ the step pattern or ramp pattern to model the pressure and flow variations in pressure/volume-controlled ventilation. It was observed that the above waveforms tend to add to the discomfort level of patients due to the presence of jerks in derivatives of pressure/flow variations; the pressure/flow variation of air and oxygen mixture should be smooth so that the patient discomfort is kept at a minimal level. To overcome the above-mentioned drawback, a careful study of the flow/pressure simulation using a cycloidal pattern during the inhalation and exhalation phases of the breath cycle was proposed and investigated in this work. Based on transient analysis of the pressure variation simulation, it was observed that the air and oxygen mixture delivered to the patient was relatively jerk-free due to the finite values of first and second-order derivatives of pressure/flow curves. Mathematical models of the proposed simulation study of the cycloidal pattern of flow variation in both pressure/volume-controlled ventilation, are formulated and presented for use by ventilator designers. A comparative study of the simulation of step, ramp and cycloidal profiles applied to the breath cycle in a typical pressure-controlled ventilation is carried out and a marginal decrease in tidal volumes was observed in the case of cycloidal profiles for a given set of ventilator settings and the results are discussed. A typical natural breath pattern of a healthy adult was experimentally measured using a CITRIX breath analyser and the above mathematical model for the volume-controlled ventilation was found to closely describe the natural breathing process, using statistical parameters. Thus, the proposed cycloidal profile of pressure/flow variations in medical ventilators will be a better alternative, when compared to the step/ramp profiles investigated in this work; further, the proposed cycloidal profile matches closely with the natural breath pattern, based on typical experimental studies.

Keywords Ventilator waveforms, Step, Ramp, Cycloidal, PCV, VCV, Normal breathing, Mathematical modelling

Mechanical ventilation (MV) is a vital, lifesaving technique used to support patients with respiratory insufficiencies or non-functioning lungs¹. A ventilator is a medical device employed by healthcare professionals to automatically inflate the lungs of patients who are unable to breathe independently or require external breathing support. Lung inflation is achieved by precisely controlling either the volume or pressure of the delivered air and oxygen mixture. Additionally, the ventilator facilitates the mixing of air and oxygen to deliver a planned proportion of oxygen into the patient's lungs².

Among the various ventilator modes, Volume Control and Pressure Control Ventilation are the two most commonly used. Simulation studies are often employed to assess ventilator performance, as models of the respiratory system are easier to understand and experiment with than real expiratory systems. Amanda Dexter et al. validated paediatric lung models using the ASL 5000 breathing simulator, comparing the results with literature data through a t-test, and found only minimal inconsistencies. This confirmed the effectiveness of the ASL 5000 simulator³. Similarly, Robert L. Chatburn and Aude Garnerio collected data from passively ventilated adult subjects and found that the results fell within the expected range for respiratory parameters such as Compliance, Resistance, Tidal Volume, and PEEP⁴. Their study highlights that the primary goal of mechanical ventilation is to restore gas exchange and alleviate patient discomfort. Minimizing discomfort in ventilation is

¹Department of Electronics and Communication Engineering, PSG Institute of Technology and Applied Research, Coimbatore 641026, India. ²Department of Biomedical Engineering, PSG College of Technology, Coimbatore 641004, India. ³Department of Mechanical Engineering, PSG Institute of Technology and Applied Research, Coimbatore 641026, India. ✉email: deepa@psgitech.ac.in

essential to ensure that patients can breathe as naturally as possible, even while supported by a ventilator. The ventilator should not add to the burden of an already weak patient but rather support their normal breathing pattern without requiring painful adjustments. Proper synchronization of ventilator settings with the patient's natural breathing rhythm can make ventilation feel seamless, allowing for a more comfortable and supportive experience during treatment.

Figure 1. illustrates the key ventilation parameters with the help of a typical set of pressure, flow and volume waveforms which are generally used to characterize mechanical ventilation. The different ventilation parameters reported in the literature are summarized in Appendix I together with their definitions and the range of practical values for an adult^{4,5}.

Pressure controlled ventilation (PCV) vs. volume controlled ventilation (VCV)

In Pressure-Controlled Ventilation (PCV), the ventilator is set to deliver air oxygen mixture at a specific pressure. The volume of air can vary depending on the patient's needs, but the pressure remains constant. In Volume-Controlled Ventilation, the ventilator is set to deliver a specific amount of air oxygen mixture to the patient with each breath.

Pressure control ventilation delivers mechanical breaths at a set inspiratory pressure, allowing clinicians to regulate the distending pressure applied to the airways and alveoli. The volume delivered is variable and depends on the patient's inspiratory effort. The goal of this ventilation is to achieve the appropriate alveolar pressure as defined by the clinician^{6,7}. Pressure control ventilation allows the peak inspiratory pressure (PIP) to be limited to a safe level, reducing the risk of lung damage and minimizing barotrauma in patients. In contrast, volume control ventilation enables more precise control of tidal volume (V_t) delivery, ensuring the patient's physiological needs are met and minimizing the risk of over-ventilation and associated volutrauma^{8,9}.

Related literature

The literature emphasizes the critical importance of incorporating an adaptive demand flow system in medical ventilators. This system is essential for minimizing patient discomfort while ensuring precise airflow delivery, as it closely aligns with the patient's natural breathing patterns.

Roubík, Karel, et al. focused on developing and controlling a demand flow system that enables spontaneous breathing for patients connected to a High Frequency Oscillation (HFO) ventilator. Their study discusses the control strategy used in the demand flow system to regulate gas flow and pressure according to the patient's breathing patterns. This approach aims to provide appropriate ventilation support while aligning with the patient's natural respiratory rhythm¹. Mike Borrello et al. explored the implementation of adaptive control techniques for a proportional flow valve used in critical care ventilators, emphasizing the importance of delivering precise and adjustable gas flow rates to meet the respiratory needs of patients². Amanda Dexter et al. demonstrated the effective validation of lung models using the ASL 5000 breathing simulator, ensuring the accuracy and reliability of simulated respiratory parameters, ultimately enhancing the quality and applicability of lung models in various healthcare applications³.

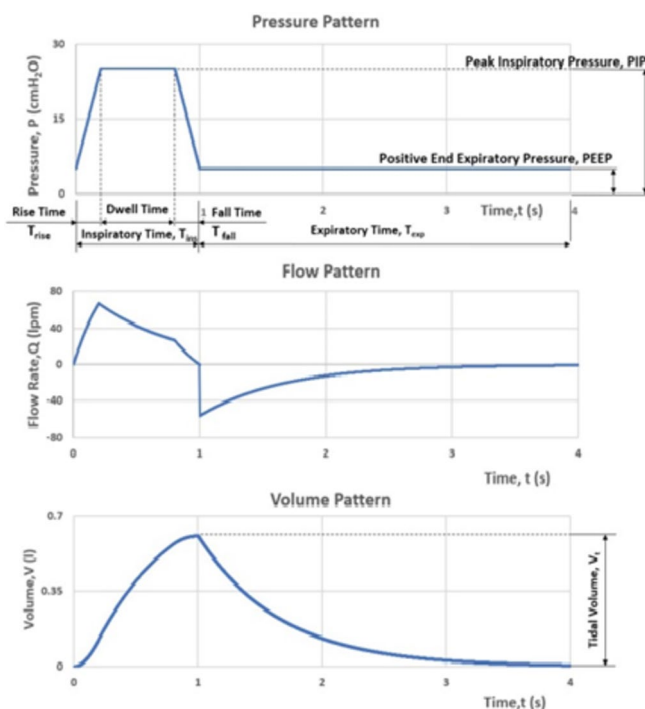


Fig. 1. A typical Ventilator waveform – Nomenclature of key parameters of ventilation.

Chatburn, in his book⁴, provides a comprehensive overview of mechanical ventilation principles and their practical applications. It details regarding the ventilator settings and parameters, including tidal volume, respiratory rate, inspiratory flow rate, inspiratory time, positive end-expiratory pressure (PEEP), and FiO₂ (Fraction of Inspired Oxygen). Strategies and interventions aimed at reducing the Work of Breathing (WoB) are discussed by Cabello in his work⁵. It emphasizes the importance of understanding WOB in assessing respiratory effort and monitoring respiratory function in critically ill patients. In their work¹⁰, the authors focus on the simulation and analysis of a mathematical model related to Pressure Controlled Ventilation (PCV). Ashworth, in his research work¹¹, discusses considerations for weaning patients from PCV based on the algorithmic approach, emphasizing gradual reductions in ventilator support while monitoring patient response and readiness for extubation.

Anitha et al. discussed the use of controlled mechanical ventilation to achieve enhanced measurements from pressure and flow sensors¹². By maintaining consistent and controlled airflow conditions, these sensors can deliver more accurate and reliable data on respiratory parameters. Rittayamai, in their article⁸, provides a detailed comparison and evaluation of pressure-controlled ventilation (PCV) and volume-controlled ventilation (VCV), focusing on their efficacy and outcomes in managing patients.

Baker, in his book elaborates the systems which leverage machine learning to dynamically sync ventilator support with the patient's natural breathing efforts, thereby reducing the discomfort caused by asynchronous ventilation. Such intelligent control systems can predict and adjust to changes in lung conditions, enabling more personalized and precise ventilation management¹³. Mohanram and Ranganathan (2024) present a fuzzy logic-based current control method for regulating proportional flow control valves in medical ventilators. The approach enhances precision in airflow management, ensuring smoother and more responsive control for patient breathing assistance¹⁴.

Methodology

This section presents the different patterns of waveforms employed in the simulation of Pressure and Volume Control Ventilation. The step, ramp and cycloidal waveforms are applied for simulating a ventilator and the results are compared and discussed. These waveforms—step, ramp, and cycloidal—define how pressure or volume changes over time during the inspiratory phase of a ventilator cycle. Each waveform has distinct characteristics that affect the distribution of airflow, patient comfort, and the overall effectiveness of ventilation.

Step and ramp pattern waveforms used in the simulation of mechanical ventilation – limitations

The step and ramp pattern waveforms used in the simulation of mechanical ventilation are presented. The step waveform is characterized by an immediate rise to the target pressure or flow rate, which is then maintained at a constant level throughout the inspiratory phase. The ramp waveform, also known as a linear waveform, features a gradual increase in pressure or flow rate over the inspiratory phase. Instead of an immediate jump, the parameter rises steadily.

Figure 2a shows a typical cycle of pressure-controlled ventilation using a step pattern. In this case, the pressure is limited to a maximum peak inspiratory pressure (PIP) of 25 cmH₂O. The inspiration cycle lasts for $T_{ins} = 1$ s, followed by the expiration cycle, which lasts for $T_{exp} = 3$ s. During inhalation, the pressure increases to PIP and during exhalation, it decreases to a plateau value of positive end-expiratory pressure (PEEP), which is 6 cmH₂O.

Figure 3a depicts pressure variation with a ramp pattern. Unlike the step pattern, the pressure gradually rises to the maximum PIP of 25 cmH₂O. The time taken for this gradual rise to PIP is referred to as T_{rise} , which in this example is 0.2 s. Similarly, during exhalation, the pressure decreases from PIP to PEEP over a duration of $T_{fall} = 0.2$ s.

Based on the step and ramp patterns, it is observed that at the changeover points, such as A1 and B1 (as shown in Fig. 2a), there is a noticeable steep change in the slope of the curve. This is depicted in Fig. 2b, where the abrupt transitions in the slope of the curve at these points are evident. In Fig. 2a, it can be observed that the pressure changes over time, as tracked by the first derivative of pressure $\frac{dP(t)}{dt}$ approaches infinity at the changeover points A2 and B2. This is illustrated in Fig. 2b, where the steep slopes at these points indicate an infinite rate of change in pressure. This phenomenon of abrupt changes in instantaneous pressure can lead to discomfort for the patient being ventilated⁹. It is important to minimize discomfort during mechanical ventilation to ensure a more comfortable and effective patient experience.

A similar sudden change in pressure can be observed in the ramp pattern, as shown in Fig. 3a. The changeover points are designated as C1, D1, E1, and F1. At these points, the first derivative of pressure $\frac{dP(t)}{dt}$ increases abruptly from 0 to 100 cmH₂O/s. The changeover values are detailed in Fig. 3b. Corresponding to the points C2, D2, E2, and F2, it can also be observed that the second derivative of pressure with respect to time $\frac{d^2P(t)}{dt^2}$ reaches values approaching infinity at the changeover points C3, D3, E3, and F3, as shown in Fig. 3c. Such significant values of the second derivative can increase patient discomfort. Therefore, it is essential for the pressure variation over time to be smooth to minimize patient discomfort.

A similar phenomenon can be observed in volume control ventilation, where the changeover points are also critical and the details are not shown here for brevity. Table 1 lists the typical ventilator parameters used in the literature^{15–17}, and the same was used in the simulation of different modes of ventilation.

Cam analogy

In the analogy of motion of a typical machine element - cam, it is essential that the profile of the cam motion be smooth so that the third derivative of displacement i.e., the jerk is minimal so that the effects of inertia are

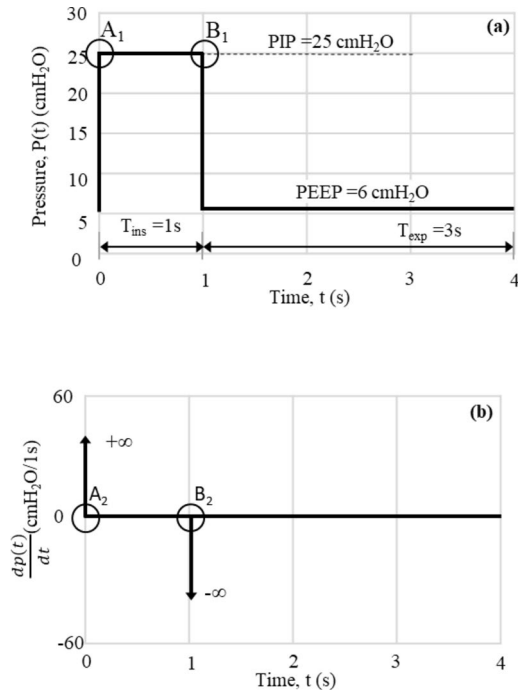


Fig. 2. Simulation of step pattern - pressure-controlled ventilation, (a) Variation of pressure, $p(t)$ for a single

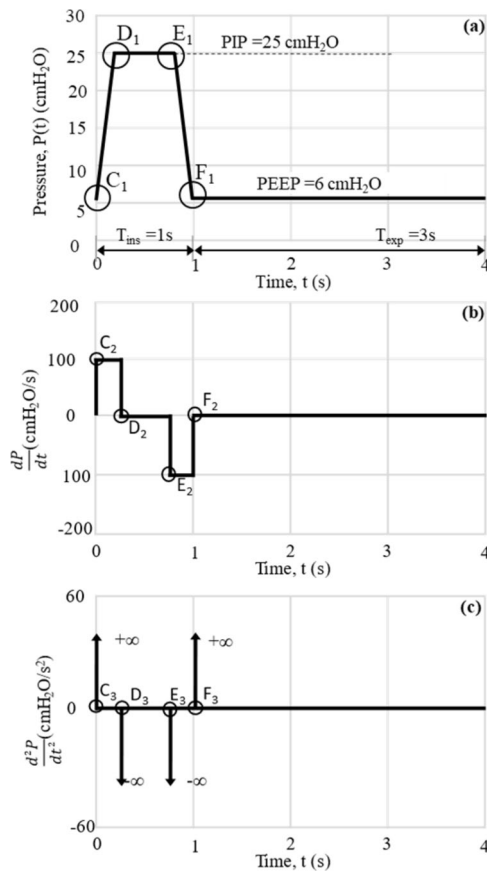


Fig. 3. Simulation of ramp pattern - Pressure-controlled ventilation, (a) Variation of Pressure, $p(t)$ for a single

Ventilator parameters	Unit	Recommended values for adults	Typical values considered for the study
Lung Compliance, C,	mL/cmH ₂ O	30 to 75	50
Resistance, R	cmH ₂ O/Lps	10 to 30	25 or 13
PIP _{max} (Peak Inspiratory Pressure)	cmH ₂ O	Below 30	25
PEEP (Positive End Expiratory Pressure)	cmH ₂ O	5 to 15	6
V _t (Tidal Volume)	mL/kg	6 to 8	7 (Age 50y)
T _{rise} (Rise Time) (% of breath cycle)	s	10–30%	10–30%
T _{fall} (Fall Time) (% of breath cycle)	s	10–30%	10–30%
RR (Respiratory Rate)	Breaths/min	12 to 20	15
Inspiratory to Expiratory Ratio	-	1:2 to 1:4	1:3

Table 1. Ventilator parameters – typical values considered for the present study as recommended in literature.

reduced, especially when the cam is operating at high velocity. Rothbart et al.¹⁸ analysed three different cam profiles, such as Simple Harmonic, Parabolic, and Cycloidal. Out of these three, the cycloidal profile was found to have a finite value of higher-order derivatives of displacement. The cycloidal profile was found to have a finite value of the third derivative, which contributes to the smoother motion of the Cam when compared to the other profiles. A similar approach has been used in mechanical ventilation so that the discomfort of the patient can be minimized due to abrupt changes in pressure and flow.

Results and discussion

Cycloidal pattern

The cycloidal waveform, also known as a sinusoidal or harmonic waveform, is characterized by a smooth, curvilinear increase and decrease in pressure or flow rate. The rise and fall follow a sinusoidal pattern, creating a wave-like delivery.

In this section, the pressure pattern in pressure-controlled ventilation is simulated using a cycloidal profile, a method widely employed in cam mechanisms. To conduct the simulation, the governing equations for pressure, flow, and volume associated with the cycloidal profile for both rise and fall segments were derived, similar to the SIVA model⁴. The graphical representations of the pressure, flow, and volume parameters are illustrated in Fig. 4a, Fig. 4b, and Fig. 4c, respectively.

The input parameters for simulating cycloidal profile, shown in Fig. 4(a), are shown in Table 2.

The equations derived for the various segments for PCV in Fig. 4 - Segment (1) to (8) are shown in Eq. (1) to Eq. (8).

$$P(t) = \frac{\Delta P_{max} * t}{T_{rise}} - \frac{\Delta P_{max}}{2\pi} \sin\left(\frac{2\pi t}{T_{rise}}\right) + PEEP \rightarrow \text{Segment 1} \quad (1)$$

$$P(t) = PIP \rightarrow \text{Segment 2} \quad (2)$$

$$P(t) = \frac{\Delta P_{max} * (T_{ins} - t)}{T_{fall}} - \frac{\Delta P_{max}}{2\pi} \sin\left(\frac{2\pi (T_{ins} - t)}{T_{fall}}\right) + PEEP \rightarrow \text{Segment 3} \quad (3)$$

$$P(t) = PEEP \rightarrow \text{Segment 4} \quad (4)$$

$$Q(t) = \frac{\Delta P(t)}{R} * e^{\left(\frac{-t}{RC}\right)} \rightarrow \text{Segment 5} \quad (5)$$

$$Q(t) = \frac{-\Delta P(t)}{R} * e^{\left(\frac{-t}{RC}\right)} \rightarrow \text{Segment 6} \quad (6)$$

$$V(t) = C * \Delta P(t) * \left[1 - e^{\left(\frac{-t}{RC}\right)}\right] \rightarrow \text{Segment 7} \quad (7)$$

$$V(t) = C * \Delta P(t) * e^{\left(\frac{-t}{RC}\right)} \rightarrow \text{Segment 8} \quad (8)$$

Efforts have been made to maintain the common input parameters identical to the ramp pattern; for example, the rise time and the fall time are maintained in 0.2 s (i.e. T_{rise}=0.2s, T_{fall}=0.2s).

Investigation of derivatives of cycloidal profile

A detailed examination of the simulation results for the cycloidal pattern of pressure-controlled ventilation, as depicted in Fig. 5a, identifies specific transition points where the cycloidal profile undergoes significant alterations, particularly highlighted in Fig. 5b. These transition points occur within the pressure range of 6 to 25 cmH₂O. When the first and second derivatives of the profile are scrutinized to evaluate potential discomfort experienced by the patient, it is evident from Fig. 5b that the first derivative shows a gradual variation. This gradual change implies that the patient is likely to experience minimal discomfort during these transitions. Not only does the first derivative change gradually, but the second derivative, as illustrated in Fig. 5b, also exhibits

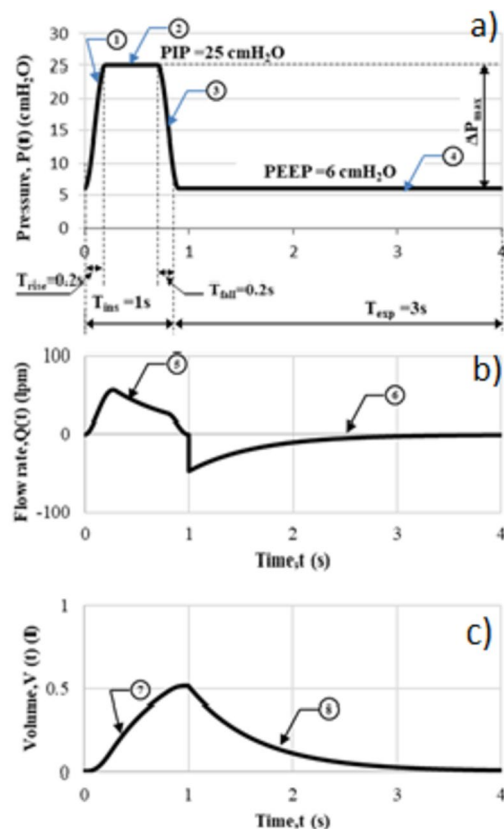


Fig. 4. Simulation using cycloidal profile – PCV, (a) Pressure pattern (b) Flow pattern (c) Volume pattern.

Parameter	Set value
Profile	Cycloidal
Inspiration time, T_{ins}	1.00 s ($T_{rise}=0.2s, T_{fall}=0.2s$)
Expiration time, T_{exp}	3.00 s
Peak inspiratory pressure, PIP	25.00 cmH ₂ O
Airway resistance, R^*	13.00 cmH ₂ O/lps
Lung compliance, C^*	50 ml/ cmH ₂ O

Table 2. The input parameters applied to the cycloidal profile. *Typical values for an adult, that have been used in computation for discussion.

a gradual variation during the inhalation phase, rise time, and fall time. Specifically, the peak value of the first derivative $\frac{dP(t)}{dt}$, is 149 cmH₂O/s [Fig. 5b], while the peak value of the second derivative $\frac{d^2P(t)}{dt^2}$, is limited to 2,341 cmH₂O/s² [Fig. 5c]. These values are finite, contrasting with the infinite values observed in step and ramp patterns, respectively. This clearly demonstrates that the cycloidal profile effectively limits the peak values of both first and second-order derivatives.

During both inhalation and exhalation phases, the profiles and their derivatives exhibit gradual transitions, as shown in Fig. 5a,b,c. Consequently, such a cycloidal pattern could be optimally employed in the simulation of pressure-controlled ventilation for patients utilizing medical ventilators.

The higher values in the derivatives of STEP and RAMP ($\pm \infty$) as shown in Table 3 add to the discomfort of the patient. However, corresponding values in the case of cycloidal pattern is limited to a finite value. Thus, the analysis demonstrated that the cycloidal pattern results in a relatively jerk-free delivery of air and oxygen mixtures, thanks to the finite values of the derivatives in the pressure and flow curves.

The pressure, volume, and flow pattern curves in pressure-controlled ventilation using three distinct pressure shapes—step, ramp, and cycloidal—are illustrated in Fig. 6a. The relevant parameters for the pressure-controlled ventilation were set as follows: $T_{ins} = 1$ s, $T_{exp} = 3$ s, $T_{rise} = T_{fall} = 0.2$ s, Peak Inspiratory Pressure (PIP) = 25 cmH₂O, and Positive End-Expiratory Pressure (PEEP) = 6 cmH₂O. It is observed that the tidal volumes delivered in the ramp and cycloidal shapes are not significantly different, with a slight reduction of 0.746 ml compared to the step shape, as shown in Fig. 6b. This difference is attributed to the reduced flow rate requirement, as indicated in

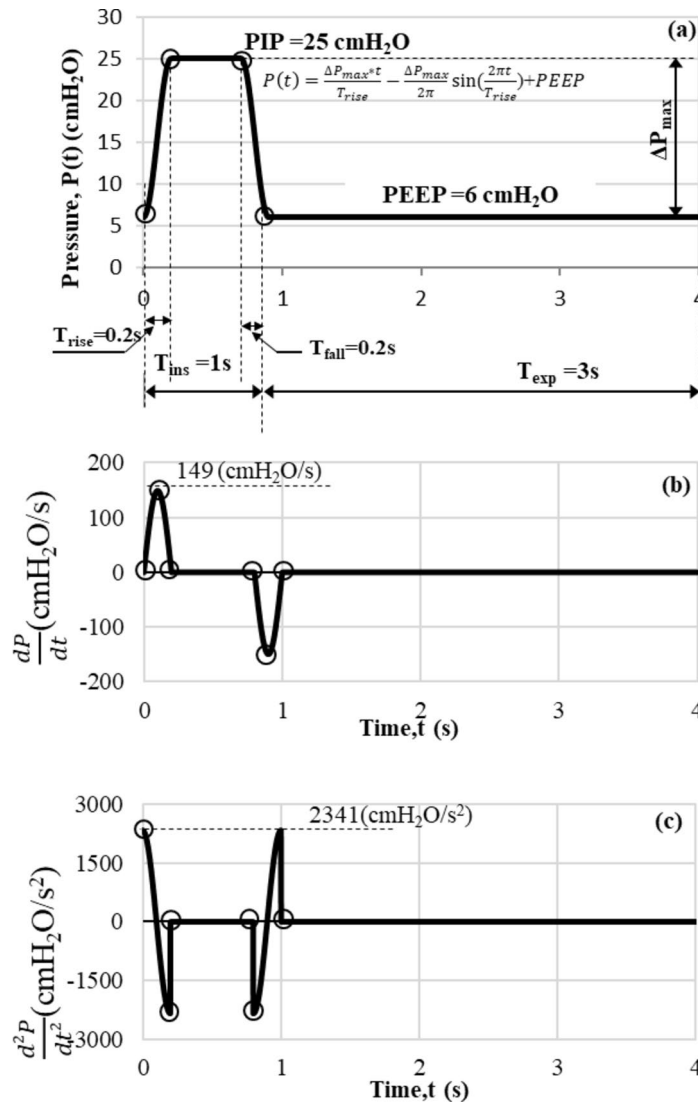


Fig. 5. Transient analysis - Simulation using Cycloidal profile (PCV), (a) Pressure Variation for a single breath cycle, (b) Variation of $\frac{dP(t)}{dt}$ for a single breath cycle, (c) Variation of $\frac{d^2P(t)}{dt^2}$ for a single breath cycle

Derivatives of pressure	STEP	RAMP	Cycloidal
Breath pattern			
Transition points	A ₁ , B ₁	C ₁ , D ₁ , E ₁ , F ₁	X ₁ , Y ₁
$\left(\frac{dP}{dt}\right)_{max}$	$\pm \infty$ (A ₁ , B ₁)	± 100 cmH ₂ O/s (D ₁ , E ₁)	± 149 cmH ₂ O/s (X ₁ , Y ₁)
$\left(\frac{d^2P}{dt^2}\right)_{max}$	---	$\pm \infty$ (C ₁ , D ₁ , E ₁ , F ₁)	± 2341 cmH ₂ O/s ² (X ₁ , Y ₁)

Table 3. Comparison of peak values of derivatives of STEP, RAMP & cycloidal waveforms at the transition points (for example pressure variation in PCV) for a given set of ventilator parameters.

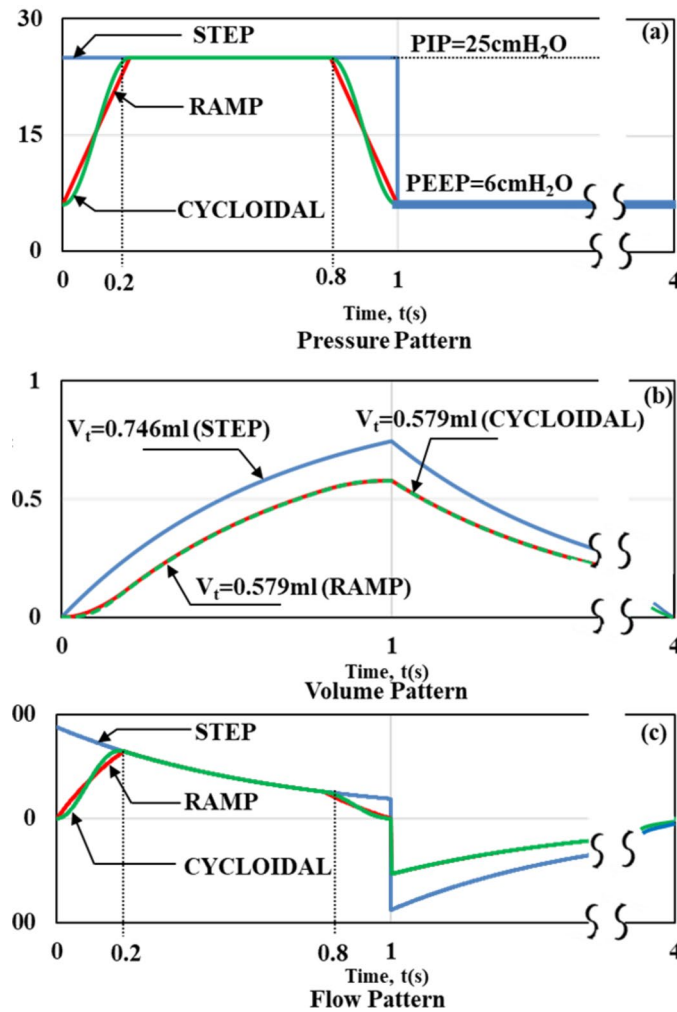


Fig. 6. Comparison and analysis of Step, Ramp and Cycloidal profiles – PCV, (a) Pressure pattern (b) Volume pattern (c) Flow pattern.

Fig. 6c, which is necessary to maintain a gradual rise in the pressure pattern, as depicted in Fig. 6a. Consequently, the proposed cycloidal curves for the pressure pattern in pressure-controlled ventilation demonstrate a smoother transition, reducing the likelihood of jerks compared to the step and ramp forms, although there is a marginal decrease in tidal volume to 0.579 ml for the same ventilator parameter settings.

Similar studies were extended to the simulation of volume-controlled ventilation using cycloidal profile for the inhalation phase as shown in Fig. 7. The typical input data for the above simulation purpose is shown in Table 4.

The equations derived for the various segments for VCV in Fig. 7 - Segment (1) to (8) are shown in Eq. 9 to Eq. 16.

$$Q(t) = \frac{Q_{max} * t}{T_{rise}} - \frac{Q_{max}}{2\pi} \sin\left(\frac{2\pi t}{T_{rise}}\right) \rightarrow \text{Segment 1} \tag{9}$$

$$Q(t) = Q_{max} \rightarrow \text{Segment 2} \tag{10}$$

$$Q(t) = \frac{Q_{max} * (T_{ins} - t)}{T_{fall}} - \frac{Q_{max}}{2\pi} \sin\left(\frac{2\pi (T_{ins} - t)}{T_{fall}}\right) \rightarrow \text{Segment 3} \tag{11}$$

$$Q(t) = \frac{-V_t}{RC} * e^{\left(\frac{-t}{RC}\right)} \rightarrow \text{Segment 4} \tag{12}$$

$$V(t) = \int Q(t) dt \rightarrow \text{Segment 5} \tag{13}$$

$$Q(t) = V_t * e^{\left(\frac{-t}{RC}\right)} \rightarrow \text{Segment 6} \tag{14}$$

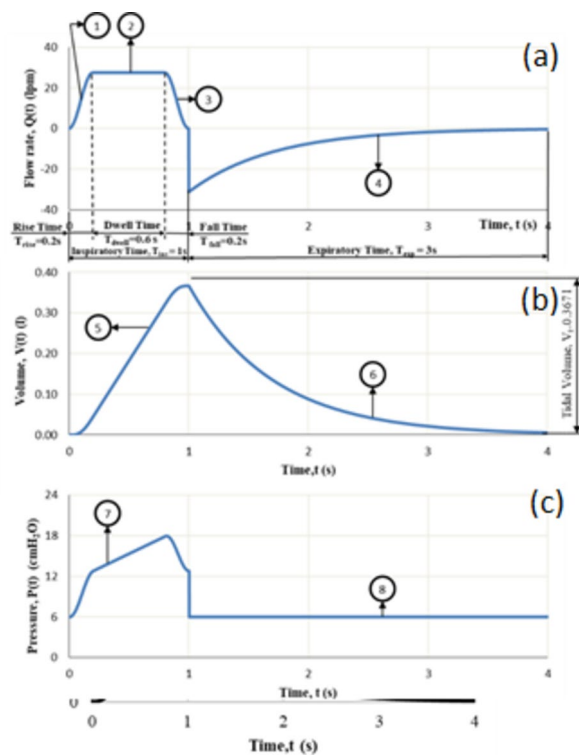


Fig. 7. Flow, Volume and Pressure patterns for Volume Controlled Ventilation.

Parameter	Set value
Profile	Cycloidal
Inspiration time, T_{ins}	1.00 s ($T_{rise}=0.2s, T_{fall}=0.2s$)
Expiration time, T_{exp}	3.00 s
Maximum flow rate, Q_{max}	27.51 lpm
Tidal volume, V_t	0.367 l
Peak end exhalatory pressure, PEEP	6.00 cmH ₂ O
Airway resistance, R^*	13.00 cmH ₂ O/lps
Lung compliance, C^*	54 ml/ cmH ₂ O

Table 4. The input parameters for volume-controlled ventilation. *Typical values for an adult, that have been used in computation for discussion.

$$P(t) = E * V(t) + R * Q(t) + PEEP \rightarrow \text{Segment 7} \tag{15}$$

$$P(t) = PEEP \rightarrow \text{Segment 8} \tag{16}$$

Normal breathing curve

To experimentally determine the breathing pattern of a normal, healthy adult, an experimental setup was constructed in the laboratory, as illustrated in Fig. 8.

The (air + oxygen) flow data, both input and output, during the inhalation and exhalation phases of the individual were recorded using the Breath Analyser (Model No. CITRIX H4). This device is equipped with an output feature that allows digital data to be captured and subsequently analyzed on a PC.

A typical natural breathing curve of a healthy individual, experimentally measured, is presented in Fig. 9. It can be observed that this natural breath pattern closely resembles the curve seen in volume-controlled ventilation, as shown in Fig. 6. Consequently, the subsequent mathematical modeling was performed using a cycloidal profile for the rise and fall segments and a ramp pattern for the dwell segments of the volume-controlled ventilation. The experimentally measured flow and volume parameters corresponding to this typical breath pattern are detailed in Table 5.

The flow pattern was subsequently modelled using cycloidal profiles for the T_{rise} and T_{fall} segments (specifically segments N1, N3, N4, and N6) of the inspiration and expiration phases. The model results were then compared with the actual flow data, as shown in Fig. 10. Curve fitting was performed using the Pearson Product Moment



Fig. 8. Experimental setup for capturing the normal breathing pattern.

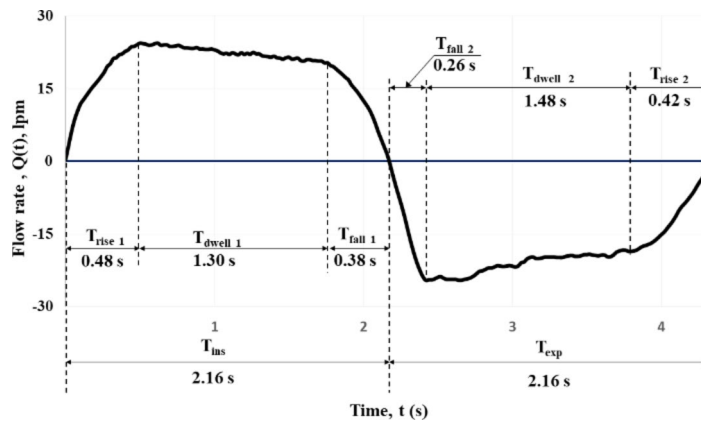


Fig. 9. Flow rate vs. Time graph – Natural Breathing.

Parameter	Value
Inspiration phase, $T_{ins}=2.160$ s	Rise Time, T_{rise1} 0.48 s
	Dwell Time, T_{dwell1} 1.30 s
	Fall Time, T_{fall1} 0.38 s
Expiration phase, $T_{exp}=2.160$ s	Fall Time, T_{fall2} 0.26 s
	Dwell Time, T_{dwell2} 1.48 s
	Rise Time, T_{rise2} 0.42 s
Maximum flowrate, Q_{max1}	24.33lpm
Tidal volume, V_t	0.672 l

Table 5. The measured parameters for natural breath pattern.

Correlation method⁹, and the coefficient of determination (r^2) for the curve fitting process was established at 98%. This r^2 value is considered satisfactory, as it exceeds the minimum recommended value of 95% for goodness of fit. The high r^2 value confirms the adequacy of the cycloidal pattern used in modelling the breathing curve for Volume-Controlled Ventilation.

The extracted flow equations for the inhalation and exhalation phases, following the cycloidal pattern are shown in Eq. (17) to Eq. (22).

The maximum and minimum values of flow during inhalation ($Q_{max1} = 24.33$ lpm and $Q_{max2} = 22.24$ lpm) and exhalation are shown in Fig. 10.

$$Q(t) = 50.79t - 3.87 * \sin(13.12 t) \quad N1 \tag{17}$$

$$Q(t) = -1.61(t - 0.48) + 24.33 \quad N2 \tag{18}$$

$$Q(t) = 58.52(2.16 - t) - 3.54 * \sin(16.53 * (2.16 - t)) \quad N3 \tag{19}$$

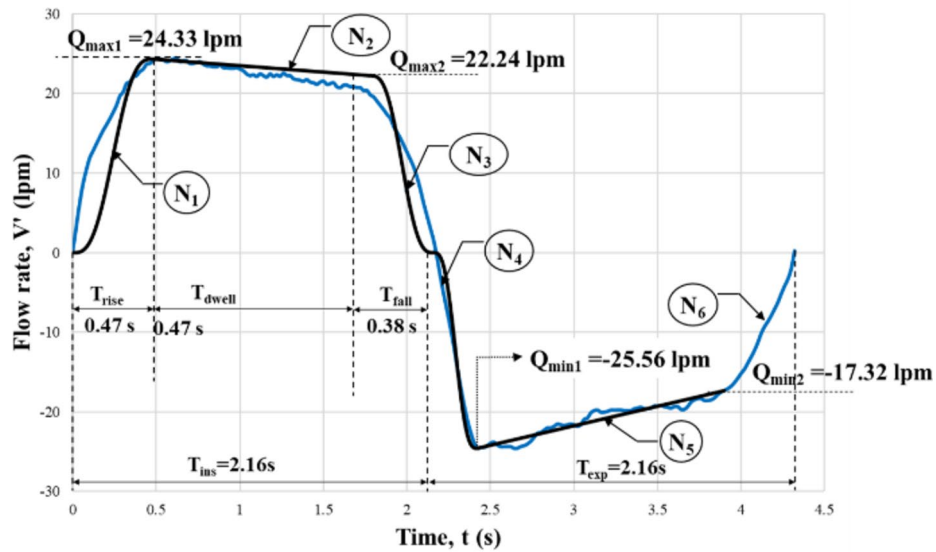


Fig. 10. Modelling of natural breath pattern using cycloidal profile (N1 – N6).

Parameter	Value	
Inspiration phase, $T_{ins} = 2.160$ s	Rise time, T_{rise1}	0.47 s
	Dwell time, T_{dwell1}	1.31 s
	Fall time, T_{fall1}	0.38 s
Maximum flowrate, Q_{max1}	24.33 lpm	

Table 6. Mapping operational parameters from Cycloidal Profile to Natural Breath Pattern.

$$Q(t) = -94.47 * (2.16 - t) + 3.91 * \sin(24.17 * (2.16 - t)) \quad N4 \tag{20}$$

$$Q(t) = 4.89 * (t - 2.42) - 24.56 \quad N5 \tag{21}$$

$$Q(t) = -41.24 * (t - 4.32) + 2.76 * \sin(14.96 * (t - 4.32)) \quad N5 \tag{22}$$

The usefulness of the above simulation results lies in their potential to optimize the inhalation flow characteristics of medical ventilators. This study provides valuable insights for designers of medical ventilators, enabling them to tailor different waveforms to better match the inhalation flow patterns needed for their patients.

Measured operational parameters

The operational parameters obtained from modelling the natural breath pattern using the cycloidal profile during the various phases, as illustrated in Fig. 10, are summarized in Table 6.

The lung parameter values used in the modelling to ensure an accurate match between the modelled curve and the actual breath profile:

$$R = 19.8 \text{ cmH}_2\text{O/lps}, C = 75 \text{ ml/cmH}_2\text{O}.$$

$$\text{Inferred value of PIP} = 21.4 \text{ cmH}_2\text{O}.$$

The natural breathing curve, as shown in Fig. 11, exhibits minimal transient effects. Figure 11b, c display the transient analysis of the first and second derivatives of the flow rate for the natural breathing curve, as obtained from the Breath Analyser. The results indicate that the peak derivatives are finite.

$$\left[\left(\frac{dQ}{dt} \right)_{max} = 147.7 \text{ lpm/s}; \left(\frac{d^2Q}{dt^2} \right)_{max} = 7385 \text{ lpm/s}^2 \right].$$

The cycloidal profile offers several advantages in respiratory systems, particularly for assisted ventilation. It reduces jerk, ensuring smooth transitions in airflow, which minimizes strain on lung alveoli and provides a comfortable breathing experience. The continuous flow pattern decreases effort required for breathing, protecting delicate lung tissues. This efficient airflow enhances lung filling capacity, allowing for more oxygen intake with each breath. Overall, the cycloidal profile optimizes patient comfort and breathing efficiency, making it highly suitable for medical ventilation applications.

Further study has been conducted in order to improve the mathematical model of the breath patterns and a hybrid model with combined cycloidal and parabolic curve pattern was investigated and the results are shown in Fig. 12.

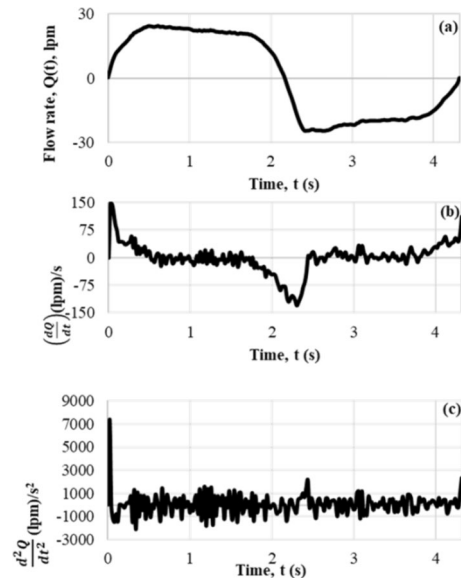


Fig. 11. Transient analysis of flow rate of a typical natural breath, (a) Flow rate $Q(t)$ - Natural breathing, (b) First Derivative of flow rate, $\frac{dQ}{dt}$, (c) Second derivate of flow rate, $\frac{d^2Q}{dt^2}$

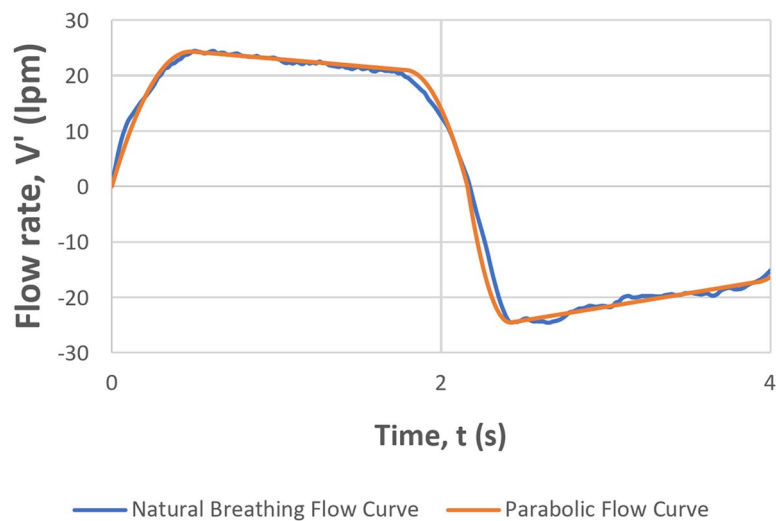


Fig. 12. Modelling of natural breath using parabolic profile

Conclusion

This study explores the complexities of pressure and volume-controlled ventilation in medical ventilators, with a focus on waveform simulations and their impact on patient comfort. A review of existing literature and simulations using step and ramp patterns revealed that these waveforms often cause patient discomfort due to abrupt pressure and flow variations. To mitigate this issue, the study introduced and examined the use of a cycloidal pattern for the inhalation and exhalation phases, aiming for smoother transitions in pressure and flow and the same was verified. The mathematical models developed offer valuable insights for ventilator designers, presenting a viable alternative to traditional step and ramp profiles. While a comparative study shows a slight decrease in tidal volume with cycloidal profiles, they maintain alignment with natural breathing patterns. The cycloidal profile thus emerges as a promising solution, enhancing patient comfort and closely resembling natural breath patterns.

Data availability

The data generated and analyzed during this study are presented in the manuscript as waveforms. Standard waveforms and their mathematical modelling have been utilized to enhance patient comfort, with a focus on the derivatives of these standard waveforms.

Received: 1 July 2024; Accepted: 8 January 2025

Published online: 15 January 2025

References

- Roubik, K., Ráfl, J., van Heerde, M. & Markhorst, D. G. Design and control of a demand flow system assuring spontaneous breathing of a patient connected to an HFO ventilator. *IEEE Trans. Biomed. Eng.* **58** (11), 3225–3233 (2011).
- Borrello, M. Adaptive control of a proportional flow valve for critical care ventilators. In 2018 Annual American Control Conference (ACC) (pp. 104–109). IEEE. (2018), June.
- Dexter, A., McNinch, N., Kaznoch, D. & Volsko, T. A. Validating lung models using the ASL 5000 breathing simulator. *Simul. Healthc.* **13** (2), 117–123 (2018).
- Chatburn, R. L. *Fundamentals of Mechanical Ventilation: A Short Course in the Theory and Application of Mechanical Ventilators* (Mandu, 2003).
- Cabello, B. & Mancebo, J. Work of breathing. *Intensive Care Med.* **32**, 1311–1314 (2006).
- Angus, D., Finfer, S., Gattioni, L. & Singer, M. *Oxford Textbook of Critical Care* (Oxford University Press, 2019).
- Park, H. & Park, D. Y. Comparative analysis on predictability of natural ventilation rate based on machine learning algorithms. *Buuld. Environ.* **195**, 107744 (2021).
- Rittayamai, N. et al. Pressure-controlled vs volume-controlled ventilation in acute respiratory failure: a physiology-based narrative and systematic review. *Chest* **148** (2), 340–355 (2015).
- Marini, J. J., Crooke, P. S. 3rd & Truitt, J. D. Determinants and limits of pressure-preset ventilation: a mathematical model of pressure control. *J. Appl. Physiol.* **67** (3), 1081–1092 (1989).
- Deepa, M. M., Vidhyapriya, R., Aparna, M. K. & Yeswantra, M. R. Simulation of mathematical model of pressure controlled ventilation (PCV). *Solid State Technol.* **63** (5), 5724–5732 (2020).
- Ashworth, L. et al. Clinical management of pressure control ventilation: an algorithmic method of patient ventilatory management to address forgotten but important variables. *J. Crit. Care.* **43**, 169–182 (2018).
- Anitha, T. & Gopu, G. Controlled mechanical ventilation for enhanced measurement in pressure and flow sensors. *Measurement: Sens.* **16**, 100054 (2021).
- Baker, D. J. Artificial ventilation in the intensive care unit: an overview. In: Artificial ventilation. Springer, Cham. https://doi.org/10.1007/978-3-030-55408-8_11 (2020).
- Mohanram, D. & Ranganathan, V. Fuzzy Logic-based current control logic for proportional flow control valve system of medical ventilators. In *Proceedings of the Bulgarian Academy of Sciences* (Vol. 77, No. 9, pp. 1331–1339). (2024), September.
- Amato, M. B. et al. Driving pressure and survival in the acute respiratory distress syndrome. *N. Engl. J. Med.* **372** (8), 747–755 (2015).
- Gattinoni, L. et al. Intensive care medicine in 2050: ARDS. *Intensive Care Med.* **42** (1), 73–82 (2016).
- ARDSNet Ventilation with lower tidal volumes as compared with traditional tidal volumes for acute lung injury and the acute respiratory distress syndrome. *N. Engl. J. Med.* **342** (18), 1301–1308 (2000).
- Rothbart, H. A. & Eng, D. Polynomial series cam and curves fourier. *Cam Design Handbook*, 89. (2004).

Acknowledgements

We wish to acknowledge the management of PSG Institute of Technology and Applied Research for supporting throughout the research study.

Author contributions

All authors have reviewed the revised manuscript before the submission.

Declarations

Competing interests

The authors declare no competing interests.

Additional information

Supplementary Information The online version contains supplementary material available at <https://doi.org/10.1038/s41598-025-86187-5>.

Correspondence and requests for materials should be addressed to M.D.

Reprints and permissions information is available at www.nature.com/reprints.

Publisher's note Springer Nature remains neutral with regard to jurisdictional claims in published maps and institutional affiliations.

Open Access This article is licensed under a Creative Commons Attribution-NonCommercial-NoDerivatives 4.0 International License, which permits any non-commercial use, sharing, distribution and reproduction in any medium or format, as long as you give appropriate credit to the original author(s) and the source, provide a link to the Creative Commons licence, and indicate if you modified the licensed material. You do not have permission under this licence to share adapted material derived from this article or parts of it. The images or other third party material in this article are included in the article's Creative Commons licence, unless indicated otherwise in a credit line to the material. If material is not included in the article's Creative Commons licence and your intended use is not permitted by statutory regulation or exceeds the permitted use, you will need to obtain permission directly from the copyright holder. To view a copy of this licence, visit <http://creativecommons.org/licenses/by-nc-nd/4.0/>.

© The Author(s) 2025